Rain droplet impact stress analysis for leading edge protection coating systems for wind turbine blades

T.H. Hoksbergen [*], R. Akkerman, I. Baran

University of Twente, Drienerlolaan 5, Enschede, 7522NB, The Netherlands

ARTICLE INFO

ABSTRACT

The energy transition requires clean energy production for which offshore wind shows high potential. The blade length of offshore wind turbines is currently exceeding 100 m with corresponding tip speeds of above 100 m s^{-1}. The high tip speed blades interact with airborne rain droplets which causes high pressures that lead to erosion damage over time. Protective coatings are applied based on experimental data. In order to more effectively design coating systems, the current work discusses a numerical modeling framework for predicting the stress state in multilayered co-bonded hybrid thermoplastic/thermoset coating systems. The effects on the resulting stress state were studied for changes in layer thickness, interphase thickness of the bonding zone between multiple layers, droplet diameter, coating material properties, voids and other inclusions as well as surface roughness. It was found that the design of the coating system significantly influences the dynamic stress state and as a result, the performance as a protection layer for wind turbine blades. Stress concentrations arise due to interactions of stress waves with interfaces and/or inclusions. A coating layer thickness limit was derived based on the stress concentrations and it was shown that the stress waves interact with surface defects causing fatigue crack growth around initial defects.

1. Introduction

Lowering of CO_2 emissions is crucial in global climate agreements and renewable energy is mentioned as one of the main contributors towards achieving this goal. Offshore wind energy shows high potential for producing renewable energy and meeting the electricity demands. In order to lower the levelized cost of energy, wind turbines are increasing in size to be able to harvest more energy by a larger swept area. GE installed a prototype of their Haliade-X with blades of 107 m and a rated capacity of 12 MW in 2019 in Rotterdam (the Netherlands), Siemens Gamesa announced their SG 14-236 DD with blades of 115 m to be manufactured from 2024 onward and Vestas's V236-15.0 MW uses 115.5 m blades of which a prototype was installed in 2022 in Østerild National test centre in Denmark. These longer blades result in high tip speeds that interact with airborne rain droplets which leads to high impact pressures and erosion damage over time [1]. This leading edge erosion (LEE) is causing loss in aerodynamic efficiency and a resulting lower annual energy production. This increases maintenance cost and therefore the levelized cost of energy. In order to mitigate the erosion behavior, leading edge protection (LEP) systems are being developed in the form of liquid coatings and elastomeric tapes or shells. Since damage occurs over long periods of time, modeling of rain erosion performance of the coating systems is essential in order to effectively optimize the LEP systems.

Liquid droplet impact has been studied in the aerospace, gas turbine and wind turbine sectors [1–4]. Generally, the analytical Waterhammer equation is used to estimate the contact pressure at the fluid–structure interface for a rigid solid by

$$P_{WH} = V \rho_l C_l \tag{1}$$

with V as the impact velocity, ρ_l as the density of the liquid and C_l as the acoustic velocity in the liquid. A modified version [5] has been derived that takes into account deformation of the solid domain by

$$P_{MWH} = \frac{V \rho_l C_l \rho_c C_c}{\rho_l C_l + \rho_c C_c} \tag{2}$$

with ρ_c as the density of the coating and C_c as the acoustic velocity of the coating.

Although the Waterhammer pressure is simple to calculate, it is a one dimensional simplification considering a cylinder of liquid impacting a rigid wall and therefore the physical phenomena during liquid droplet impact are not fully taken into account. Numerical methods based on combined Eulerian Lagrangian (CEL) modeling as well as smoothed particle hydrodynamics (SPH) have been developed to study
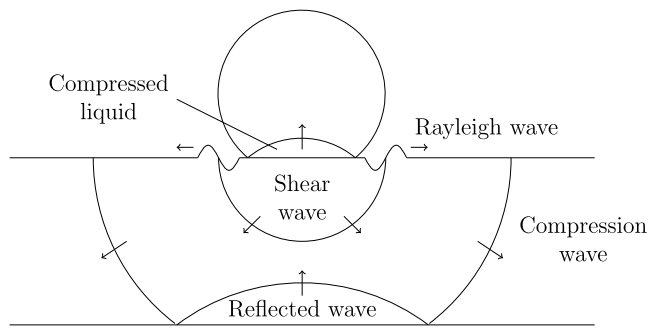
Fig. 1. Elastic waves in the substrate due to liquid droplet impact.
Source: Reproduced from [1].

the stress state in coating materials due to liquid droplet impact [6, 7]. These methods predict a local dynamic pressure that depends on the size and shape of the impacting droplet. Recently, more work towards air cushioning has been performed and a 2D axisymmetric CEL model was developed in Comsol Multiphysics® to predict the dynamic contact pressure resulting from liquid droplet impact on elastic solid targets [8].

It is well known that liquid droplet impact results in stress waves propagating in the solid target material [9]. Pressure and shear waves propagate into the bulk of the material while Rayleigh waves propagate along the surface in the radial direction as shown in Fig. 1. Depending on the material and impact properties, these waves can interact with each other and with (micro-) defects in the material which could lead to fatigue damage over time. Coating layers are applied to prevent terminal damage in the substrate. The stress state in the coating–substrate system depends on the impedance ratio between the two materials [10]. An impedance ratio close to one yields a good transmission of stress where a ratio not close to one leads to stress concentrations. Coating layers are traditionally bonded to the substrate by adhesives. Recently, other methods such as co-bonding of the coating are investigated. This method works by infusing the thermosetting resin over the coating layer which forms a functionally graded interphase between the two constituents directly. It was shown that for co-bonded polymeric materials, the bonding properties are determined by the processing conditions. A co-continuous zone can be present at the interphase between the co-bonded layers which results in a good bonding between the two components and lower stress concentrations [11–13]. Numerical modeling with a contact pressure based on SPH has shown that voids, surface defects and coating layer thickness play an important role in the stress distribution in the coating system when subjected to liquid droplet impact [7].

Lifetime prediction of coating systems has been studied based on the Palmgren–Miner rule for fatigue damage. Multiple models exist that either use the Waterhammer pressure [14,15] or numerical simulations [16–19] as input. Recently it has been shown that the lifetime prediction models based on the Waterhammer pressure show high sensitivity to changes in Poisson's ratio and material strength values which leads to an over prediction of lifetimes for certain materials [20]. For wind turbine blade coating materials based on elastomeric materials, it is therefore recommended to use methods based on accurate numerical models that are physically representative.

LEP coating materials are often based on (nanoreinforced) (T)PU materials [21]. These materials consist of hard and soft phases and segments which give the material its nano-composite like characteristic properties. TPU is a block copolymer containing hard phases which consist of a crystalline structure with some soft segments and soft phases which consist of an amorphous structure with hard segments included in the chains [22]. Phase separation occurs due to the thermodynamic incompatibility of these phases. The morphology of the TPU plays an

important role in the mechanical properties, especially the amount of hard segments, the size of the hard domains and the mixing of the hard segments into the soft domains. It was shown that polyurea and polyurethane materials respond more glass like at high strain rates than at low strain rates where they behave rubbery [23]. At high strain rates, hysteresis and cyclic softening were not observed as where at low strain rates, hysteresis was present for all samples and cyclic softening occurred for samples with crystalline hard segments but was absent for materials with amorphous well dispersed hard segments. The effect of the elastic material behavior on the resulting stress field will be further investigated in this work.

Site-specific conditions of the wind turbine operation sites are important parameters in the lifetime of the blades. It was shown that droplet diameter has an effect on the lifetime of the coating system and that the lifetime is not only shifted but also the slope of the lifetime curve changes [24]. Probabilistic models have been developed to take into account parameters such as rain droplet size distribution and wind speeds [25]. The effect of site-specific conditions on the aerodynamic properties of the eroded blades has also been investigated extensively [26]. To prevent erosion on the blades as much as possible it is therefore important to understand the performance of the coating system as well as the meteorological conditions during operation [27].

Although the liquid droplet impact response of coating materials used in wind turbines has been studied in the aforementioned literature, the influence of impact conditions, microstructure of the co-bonded region and geometrical and material parameters on the stress state development in the coating–substrate system has not been addressed. This paper is an extended version of work published in [28], which considered the effect of elastic material parameters, droplet diameter and interphase/interface description on the stress state in the coating–substrate system.

The current work further elaborates on the effect of interface and interphase definition on the stress state in the coating–substrate system. Additional studies were performed considering the effect of the elastic model, surface roughness, surface defects and inclusions on the stress state in the coating-substrate system. The stress state in the coating-substrate system as a result of liquid droplet impact predicted by the proposed model can be used in fatigue lifetime prediction models to predict leading edge protection system performance. Furthermore, a description of how the stress develops as a function of the impact pressure is presented which forms the basis for a more fundamental understanding of coating-substrate performance as leading edge erosion protection.

2. Methods

The contact pressure for liquid droplet impact on elastic solids is solved according to the numerical approach described by Hoksbergen et al. [8]. This method uses a combined Eulerian/Lagrangian description to solve the two phase flow fluid–structure interaction problem. It uses the level-set method for the two phase flow fluid domain and exports the contact pressure at the fluid–structure interface as a function of the distance to the center of impact r and time t of which an example is given in Fig. 2. The resulting contact pressure is used as input for a 2 dimensional (2D) axisymmetric simulation using the traditional Lagrangian finite element method (FEM). The two step modeling approach is valid if the reflected waves from the interface do not interact with the surface, which is the case if $h \leq \frac{C_c}{2} t_j$ where h is the applied coating thickness, C_c the acoustic velocity (pressure wave) of the coating and t_j the lateral jetting time according to

$$t_j = \frac{r_d}{V} - \frac{C_l r_d}{V\sqrt{C_l^2 + V^2}} \tag{3}$$

with r_d the droplet radius, V the impact velocity and C_l the acoustic velocity in the liquid.
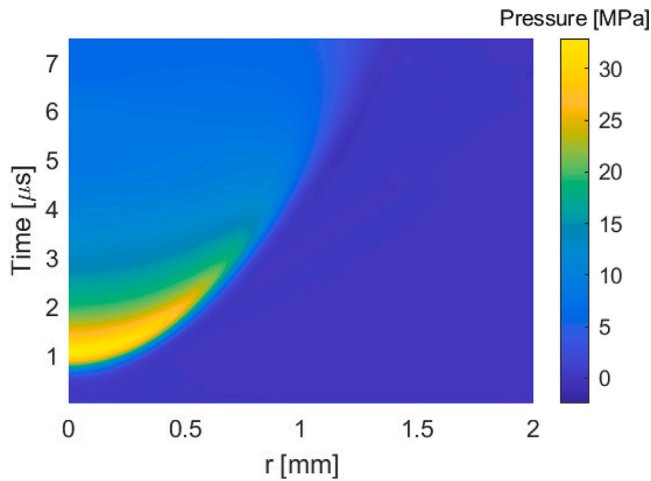
Fig. 2. Contact pressure as a function of radial coordinate and time for a 2 mm diameter water droplet impacting an epoxy target at 100 m s^{-1}.
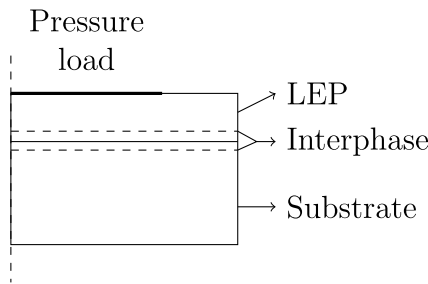

Fig. 3. Schematic overview of the problem solved by the numerical model.

The coating stress model was constructed in Comsol Multiphysics® using the solid mechanics interface with a boundary load. The implicit generalized-α solver was used with strict time stepping to solve the transient problem. The separation of the fluid–structure interaction simulation and the coating stress model was significantly reducing the computation time with respect to solving the full two phase flow problem. The model allows use of a linear elastic, hyperelastic or hyper/visco elastic isotropic material definition. Moreover, the material parameters can be defined as a function of thickness, which allows for multilayer systems with functionally graded interphase regions to be considered. For the current work, the transition region between the multiple layers is taken into account as a linear change in material properties. Using this versatile model, it was possible to study the effect of impact, geometric and material parameters on the stress field in the coating–substrate system. A schematic overview of the problem is given in Fig. 3. Slight changes to the model geometry were made to study the effect of surface roughness and voids in the coating material. Note that the axisymmetric definition limits the applicability of the model for voids, surface roughness and anisotropic materials.

The 2D axisymmetric coating stress model consists of a mapped mesh with higher mesh density towards the surface and the interfaces/interphases. The model was solved for a 3 × 3 mm material with a timestep of 10 ns and a total simulation time of 7.5 μs. The number of elements in radial direction was 75 with a quadratic bias of 5. In z-direction, the number of elements depends on the number of layers and the layer thicknesses since a denser mesh was used in the coating layer(s). For the coating layer, the number of elements was equal to the LEP thickness (in μm) divided by 10 with a quadratic bias of 2 in both directions. The amount of elements in z-direction in the substrate was equal to the substrate thickness (in μm) divided by 50 with a bias of 10.

These settings resulted in a mesh for a single coating layer of 500 μm as shown in Fig. 4.

The simulation took about 30 s to solve on a laptop with an Intel® Core™ i7-8750H and 16 GB of memory for a linear elastic material model. Since the droplet impact model took about 50 min to solve, it is highly beneficial to run these models consecutively and use the coating stress model separately to study the effects of coating thickness and interphase properties as well as the presence of voids on the stress development in the coating system, especially for an extensive parameter study. The effect of surface roughness has to be solved using the liquid droplet impact model since the fluid domain interacts directly with the surface. Also, in order to model surface roughness, cracks and voids/inclusions, triangular elements were used to more accurately describe the shapes and to allow for mesh refinement locally.

The different parameters considered for this work are given in Table 2. They were varied individually with respect to the reference case represented by the bold values. Hence, the combined effects are not considered for this work. The Von Mises stress history will be shown as slices through time or as a single time frame where the maximum stress occurred. Additionally, the dynamic stress history is provided as supplementary data in the form of GIF files. This gave insight in the development and propagation of the stress waves as well as the maximum stress state. Surface roughness was studied by applying a sine wave like surface to the coating as well as by applying a rectangular shaped surface defect. Voids and other inclusions were taken into account by considering a circular domain of 200 μm diameter in the coating layer. It should be noted in both cases that the simulation is axisymmetric and therefore these defects are not representative for real world applications. However, they do provide insight in stress concentration locations and therefore damage acceleration mechanisms.

The isotropic elastic model used for the simulations was based on either linear elasticity where Young's modulus, Poisson ratio and density were used or on a hyperelastic material model using a Neo-Hookean definition (with $n = 1$) according to

$$W = \sum_{i=1}^{n} C_{i0}(\bar{I}_1 - 3)^i + \sum_{k=1}^{n} C_{k1}(J - 1)^{2k}, \text{ where } C_{k1} = \frac{1}{D_k} \tag{4}$$

with W the strain energy density function, $\bar{I}_1$ the isochoric part of the first invariant of the right Cauchy–Green deformation tensor, J the determinant of the deformation gradient and C_{10} and D_1 given in Table 1. A hypervisco material model was possible using the hyperelastic model combined with a large-strain generalized Maxwell model for viscoelasticity, using the energy-factor β which is equivalent to $\frac{G_m}{G_\infty}$ in the small strain model for each of the branches, where G_m is the shear modulus of the corresponding branch and G_∞ is the long term shear modulus. This model is implemented using the large-strain viscoelastic definition used by Comsol Multiphysics® [29]. The current work concerns the relevance of hyperelastic and viscoelastic material models for rain erosion purposes and not obtaining exact material models. The material parameters used for the linear and hyperelastic models are summarized in Table 1 for the considered coating materials. Typically, substrates consist of anisotropic glass fiber reinforced polymer composites. The axisymmetric definition of the model does not allow these materials to be modeled. Therefore, the bulk epoxy material is used for the substrate. Because LEP layer thickness is typically high and the properties of the composite through thickness are driven by the matrix properties, this assumption is expected to not influence the results significantly. The energy factor for the considered viscoelastic material model as a function of the relaxation times is plotted in Fig. 5. This viscoelastic model is adapted to the strain rate regime of interest but is not based on a physical material.

3. Results

The dynamic Von Mises stress field solved by the model for a 2 mm liquid droplet impact on a solid epoxy target at 100 m s^{-1} is shown
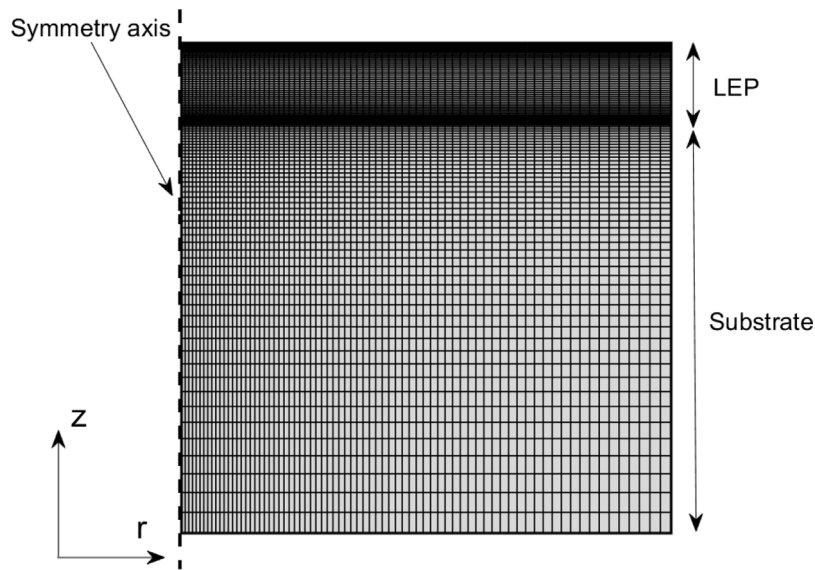
Fig. 4. Typical mesh for a coating thickness of 500 μm.

Table 1
Material parameters used for the isotropic coating systems considered in this work.

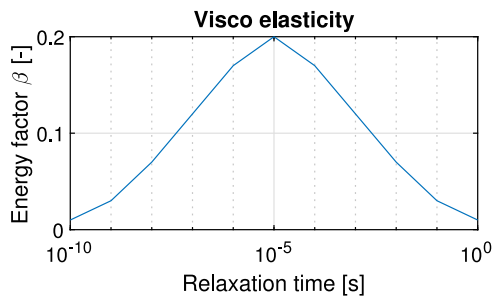| Material	TPUD60	Epoxy	PAI
E [GPa]	0.25	2.41	4.9
v [–]	0.4575	0.399	0.45
ρ [kg m^{-3}]	1100	1255	1425
C_{10} [MPa]	42.9	–	–
D_1 [MPa^{-1}]	513.8	–	–

Fig. 5. Visco elastic material parameters used for the TPUD60 coating material.

in Fig. 6. It can be seen that initially, the droplet does not make contact with the substrate and the stresses are low. At 1 μs the two materials come into contact and the central pressure starts to increase. As the impact event progresses, the stress field expands and the energy density in the stress wave disperses. This indicates that mainly the initial contact is causing high stresses and therefore this is considered for the stress analysis. It can be seen that the width of the high stress region is small compared to the droplet size. This indicates that it is very unlikely for the stress fields of two droplet impacts to interact.

The following sections focus on the effect of each individually studied parameter on the resulting stress field.

3.1. Impact velocity

Fig. 7 shows the effect of impact velocity on the stress field for 2 mm droplet impacts on an epoxy substrate. It can be seen that the stress field has a similar shape for each considered impact velocity but the magnitude changes. Moreover, the point where the highest stress is observed is located closer to the surface for higher impact velocities.

When plotting the impact velocity versus the maximum occurring Von Mises stress, it is observed that the relation is quadratic instead of linear as assumed by the Waterhammer pressure equation and corresponding stress analyses. This indicates that traditional VN-curves cannot be compared directly with SN-curves for the coating material and a more sophisticated velocity–stress relation is required.

3.2. Droplet diameter

The effect of droplet diameter on the stress field is shown in Fig. 8. It can be seen that the size and shape of the stress field change with droplet diameter. A larger droplet leads to a larger area influenced by the droplet. This also increases the depth of the volume that is affected by the maximum stress. Moreover, it is seen that the maximum stress is different for each considered droplet size where the 1 mm droplet results in the highest stress.

3.3. Material definition

Fig. 9 shows the effect of the isotropic material parameters on the frame in which the highest stress occurred during the impact event on bulk materials. The material parameters used are according to Table 1. It is observed that for the more compliant TPUD60, the stress distribution is more superficial and located in a narrower region than for both epoxy and PAI. For the stiffer PAI, the highest stress is internal and not bound to the surface. It is also seen that the material parameters influence the stress magnitude with a general consensus that more compliant materials lead to lower stresses. Depending on the material parameters, the stress develops in a different way likely introducing different failure mechanisms, lifetimes and interactions with defects and interfaces.

Also, the constitutive model used for the coating material has an effect on the predicted stress development as shown in Fig. 10. The linear elastic and hyperelastic material models show comparable stress responses. For this particular viscoelastic material model, the strain rate is affecting the stress field which is more spread out and disperses faster. The magnitudes and shapes of the stress fields being similar indicates that damage, and therefore lifetime, for these material models is expected to be similar as well. This indicates that for the used viscoelastic model at the strain rates occurring during liquid droplet impact, the material behavior is comparable to a linear elastic response. If multiple impacts are occurring with a short time in between, stress relaxation due to viscoelasticity might start to play a role which could lead to a lower lifetime of the material.

Table 2
Summary of the parameters studied in this work. The bold parameters represent the reference case.

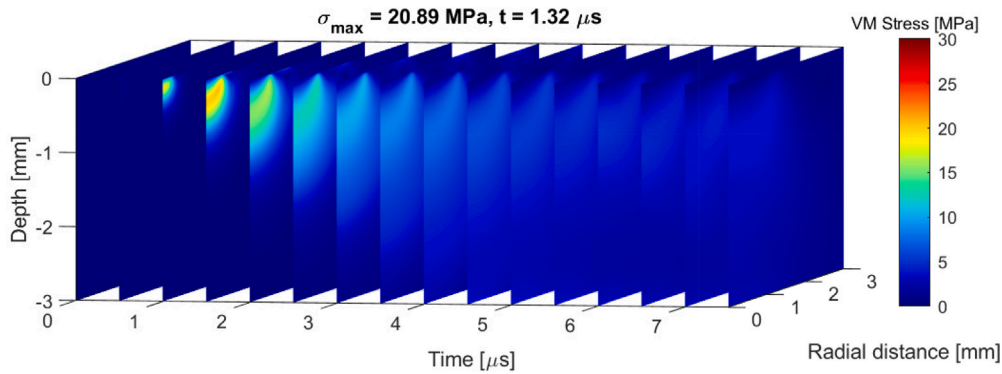| Elastic model	Impact velocity	Droplet diameter	LEP thickness	Interphase thickness	Surface roughness	Inclusion
[–]	[m s^{-1}]	[mm]	[μm]	[μm]	[–]	[–]
Linear	80	1	250	**0**	yes	**none**
Hyper	**100**	**2**	500	50	**no**	void
Hyper–visco	120	3	750	100	crack	hard
–	140	–	∞	–	–	–
–	160	–	–	–	–	–

Fig. 6. Stress history in an epoxy target for a 2 mm water droplet impacting at 100 m s^{-1}.
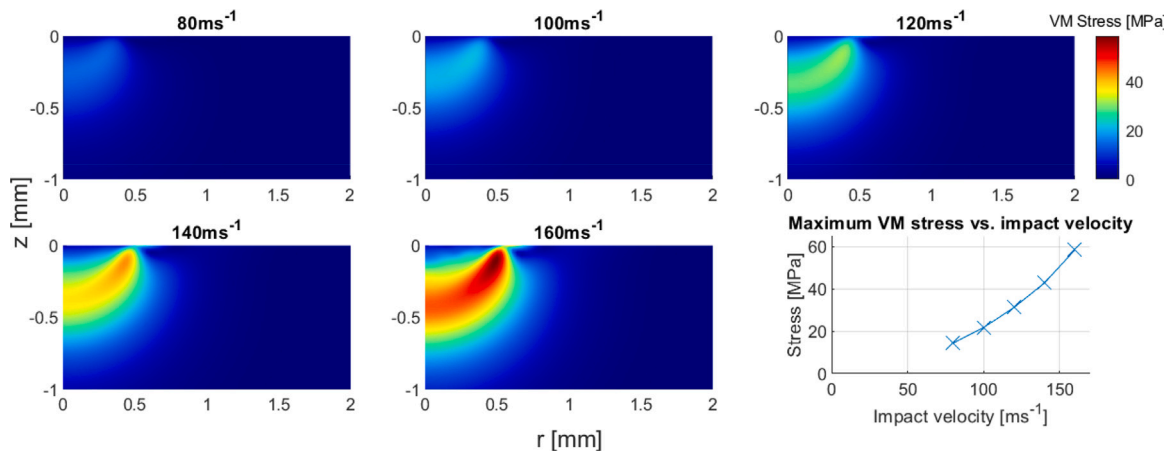

Fig. 7. Effect of impact velocity on the stress field (MPa) at the time frame where the highest Von Mises stress occurred and the relation between impact velocity and the maximum occurring Von Mises stress for 2 mm water droplet impacts on an epoxy target.
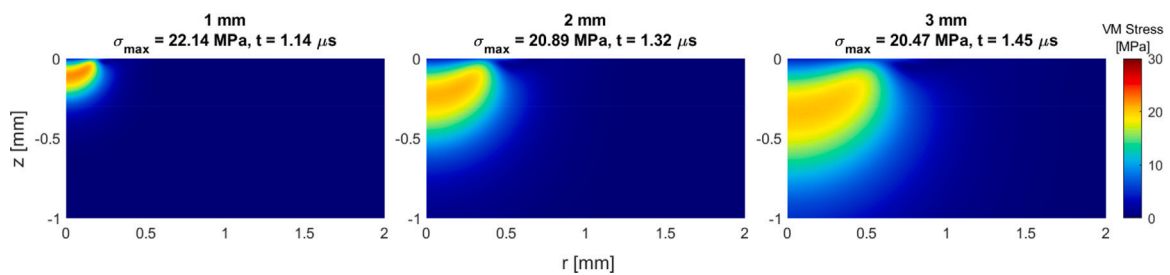

Fig. 8. Effect of droplet diameter on the stress field for water droplet impact on an epoxy target at 100 m s^{-1} at the time frame where the highest Von Mises stress occurred. The dynamic stress fields are available as supplementary GIF files.

3.4. LEP layer thickness and interphase thickness

Coating thickness plays a role in the stress distribution due to interactions of the stress field with the interface. It can be seen from Fig. 11 that the stress in both considered materials acts in a different way with the interface, represented by the solid line. The more compliant

TPUD60 material shows a high stress at the interface at some distance from the center of impact and for slightly thicker LEPs, there is a stress concentration due to the reflected wave at the center of the LEP. The PAI material shows high stresses for reflected waves directly above the interface. When increasing the coating thickness further, at some point, in both cases, the highest stress is no longer an effect of interactions
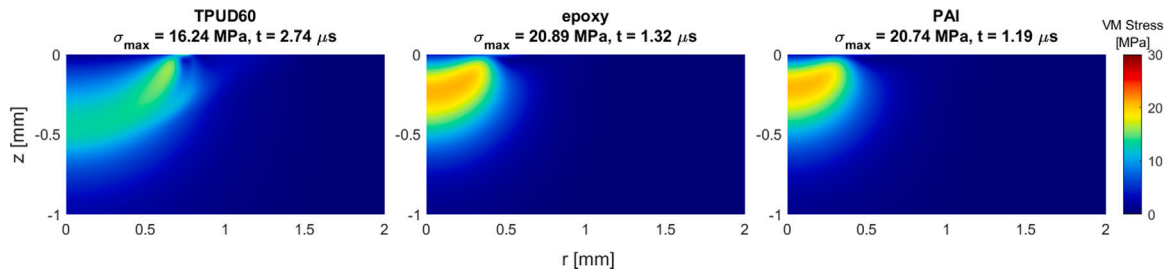
Fig. 9. The effect of material parameters on the observed stress field for 2 mm diameter water droplet impact at 100 m s⁻¹ at the time frame where the highest Von Mises stress occurred. The dynamic stress fields are available as supplementary GIF files.
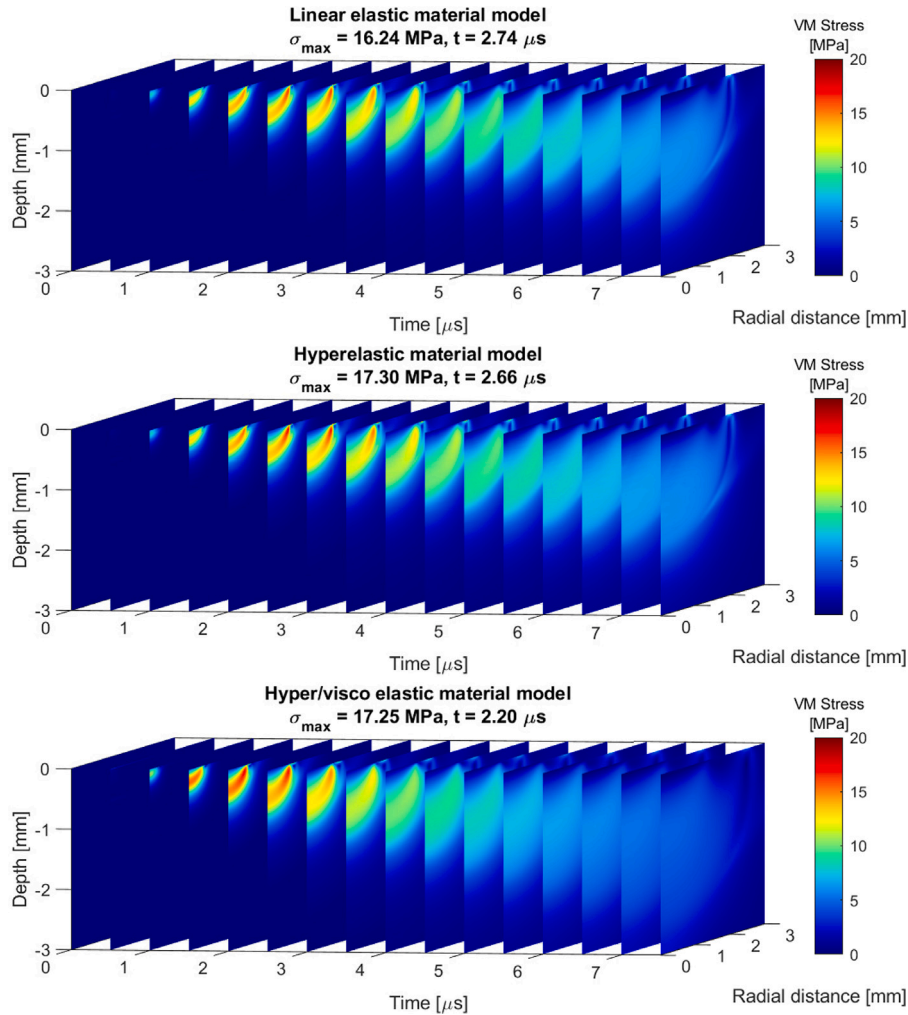

Fig. 10. Effect of the used material model on the stress field in a TPUD60 material as a result of a 2 mm water droplet impact at 100 m s⁻¹. The dynamic stress fields are available as supplementary GIF files.

with the interface but rather due to the initial wave. The resulting stress field is therefore similar to that in bulk materials which was given in Fig. 9. For thin LEP layers, it can be observed that due to interactions with the interface, the stress magnitude is higher than for thick LEPs. There is a transition point where LEP thickness no longer has an effect on the maximum occurring stress which leads to a response similar to that in the bulk material.

This analysis focuses on the stress state in the material system that assumes perfect bonding between the different layers. In reality, the bonding is not perfect and delamination could occur due to normal and shear stress accumulation at the interface. Moreover, micro-defects could be present in the interphase which could initiate delamination.

Further investigation of the effect of stress accumulation at the interface as well as minimizing manufacturing defects is necessary in order to prevent delamination as much as possible.

From the previous observations it was seen that for low coating thicknesses especially, interactions of the stress waves with the interface play a major role in the stress state. Therefore, the effect of interphase thickness is studied for LEP thicknesses of 250 μm as shown in Fig. 12, where the upper and lower bounds are represented by the solid lines. The maximum stress value corresponds to the LEP layer, not the interphase region or the substrate. It can be seen that a gradual transition of material properties across the interphase could lead to a better distribution of stress across the interphase region and therefore
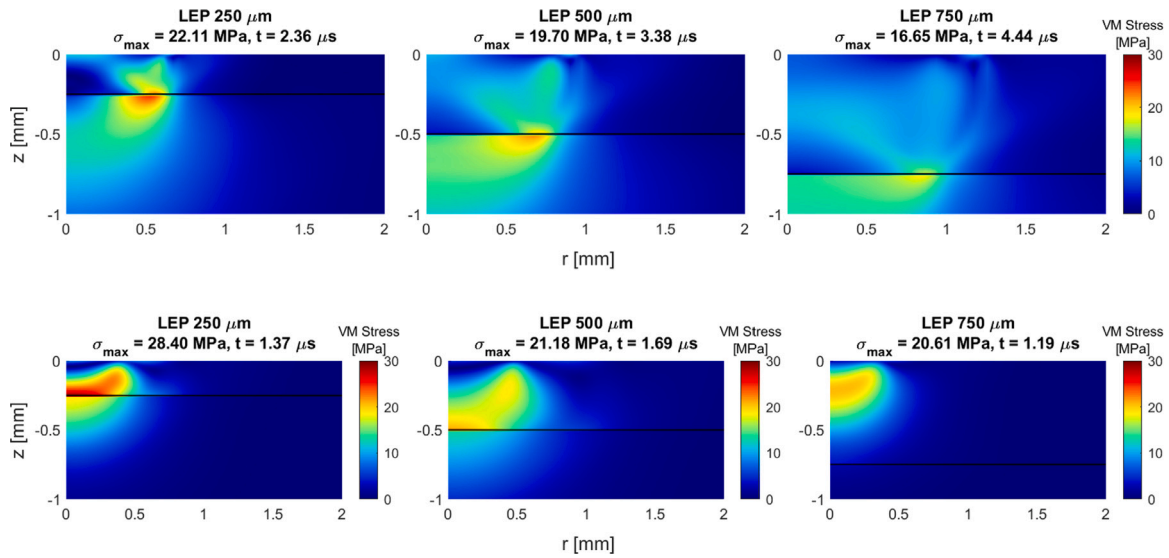
Fig. 11. Effect of material parameters and coating thickness on the stress field for TPUD60 (top) and PAI (bottom) coating materials for 2 mm diameter water droplet impact at 100 m s^{-1}. The solid line represents the interface. The dynamic stress fields are available as supplementary GIF files.
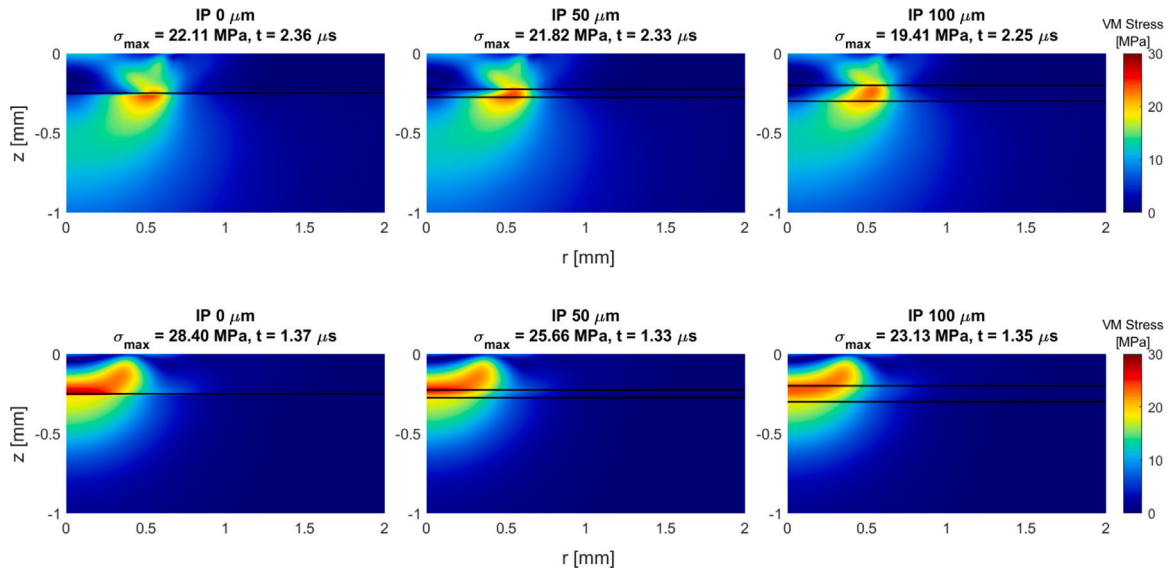

Fig. 12. Effect of interphase thickness on the stress field of TPUD60 (top) and PAI (bottom) for 2 mm diameter water droplet impact at 100 m s^{-1}. The solid lines represent the boundaries of the interphase region. The dynamic stress fields are available as supplementary GIF files.

to lower stress magnitudes. Particularly for the stiffer PAI material, where stress concentrations were caused by the compressive wave directly above the interface underneath the impact point, the gradual transition of properties across the interphase reduces the stress state in the coating layer. The elastic material parameters have been assumed to transition linearly from the coating to the substrate properties across the interphase. The effect of the transition definition on the stress propagation should be further studied.

3.5. Surface roughness and defects

Fig. 13 shows the volume fraction of water in the fluid domain (following from the level-set function) and the Von Mises stress in the solid domain for liquid droplet impact on a smooth and rough surface. It can be seen that the shape of the stress field in the solid for a rough surface is similar to that for a smooth surface. The thin layer that can be seen in between the droplet and the substrate indicates that an air layer is present in between the surface and the impacting

fluid. This air layer is acting as a lubricant for the water. Some stress concentrations arise close to the surface that could be the onset of a surface cracking damage mechanism. This could cause earlier failure due to fatigue. The effect of the level-set definition on the thickness of the lubricating air layer should be further studied since the fluid–structure interaction definition depends on the two phase flow settings. For the current level-set settings, mesh convergence is obtained.

In order to investigate the effect of surface cracking, a simulation with a square shaped surface crack was performed as shown in Fig. 14. It can again be seen that the air layer acts as a lubricant and that the lateral jets do not directly interact with the crack. The stress around the crack does however increase due to the stress waves themselves that interact with the crack. This may cause growth of the surface damage which could lead to earlier catastrophic fatigue damage.

3.6. Inclusions

The effect of the presence of a single void on the stress field is shown in Fig. 15 on the left. It is observed that stress concentrations
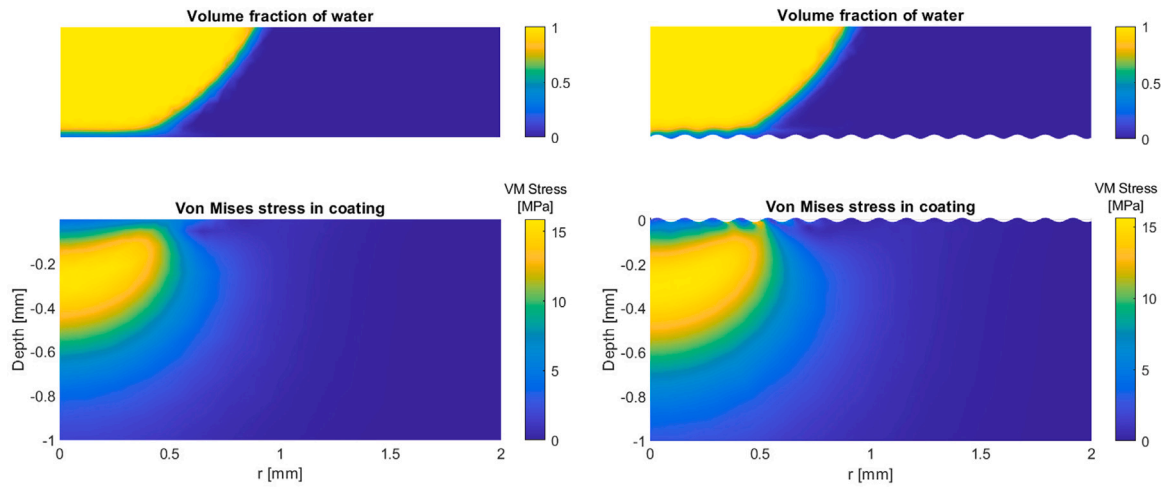
Fig. 13. Volume fraction of water in the fluid domain and Von Mises stress in the solid domain for liquid droplet impact on a smooth (left) and rough (right) surface.
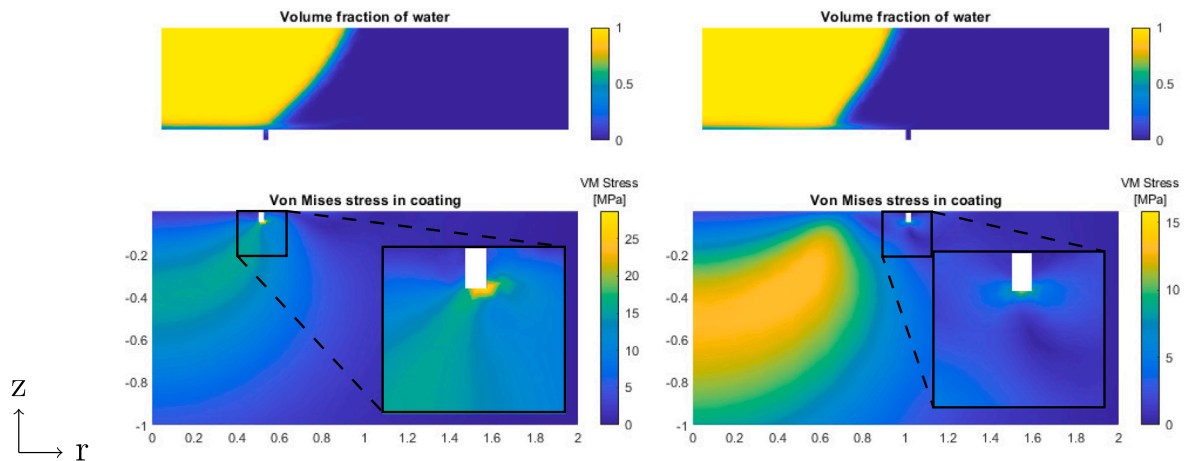

Fig. 14. Timeframe with the highest stress showing the effect of a surface crack close (left) and further away (right) from the center of impact on the stress field.

occur around this void due to the fact that the stress wave has to move around it. It should again be noted that this void is tubular shaped due to the axisymmetric definition. It is however expected that spherical voids cause similar stress concentrations. Next to the presence of voids, fibrous or particle reinforcements might be added to the material. The effect of these inclusions on the stress field is shown in Fig. 15 on the right. It can be seen that the stress concentration in the surrounding coating material is lower than in the case of a void. However, the stress transitions from a low to high value at the interface which could cause fatigue damage acceleration by debonding. In general it can be said that transitions in material properties cause stress concentrations which are likely to lead to an earlier onset of (fatigue) damage. Nano–reinforcements might be beneficial for the performance of the coating system since the stress does not interact with the inclusions at this scale and they can contribute to crack growth limitation enhancing the fatigue life.

4. Discussion

The observed stress fields are depending on material, impact and geometrical parameters. The relation between the studied parameters and the resulting stress field is not straightforward as it depends on how the stress originates and develops in the material. For a point load, the stress waves travel as given in Fig. 1, but since wavelets are continuously generated along the contact region of the droplet and the substrate, overlapping of wavelets in the substrate occurs as

shown in Fig. 16. This effect results in stress concentrations and the typical crescent stress field shape observed in the simulations of bulk materials. The time and amount of overlap depends on the contact radius velocity and the acoustic velocities in the liquid and the coating. A material with a low acoustic velocity leads to low pressures and a slow dispersion of the stress wave energy. A material with a high acoustic velocity leads to a faster dispersion of energy, but higher magnitudes for stress concentrations. An optimal material might exist that leads to a low pressure and has a relatively fast dispersion of wave energy. This material could for example be anisotropic with more compliant properties through thickness and stiffer properties in radial direction. The choice for this material however depends highly on the impact and geometric parameters indicating that the optimal LEP solution must be site specific since at different sites, droplet diameters, velocities and impact angles vary. The developed model could assist in studying the effect of changes in these parameters on the stress field which is a first step towards tailored LEP optimization.

Summarizing the results obtained so far in Table 3 (bearing in mind that the effects of the separate parameter variations are interrelated) it is clear that the performance of the LEP system highly depends on its design. Most parameters influence either the maximum stress or the size and shape of the field. Some parameters (such as LEP thickness and the LEP material parameters) affect both significantly. The effects of droplet diameter and interphase thickness are more prominent for lower LEP thicknesses due to reflections and the effect of these interrelations should be studied further.
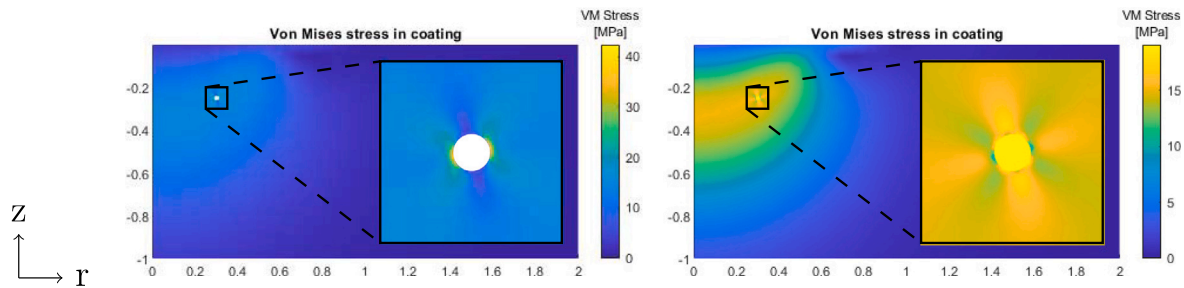
Fig. 15. The effect of voids (left) and fibrous/particle inclusions (right) on the stress field.
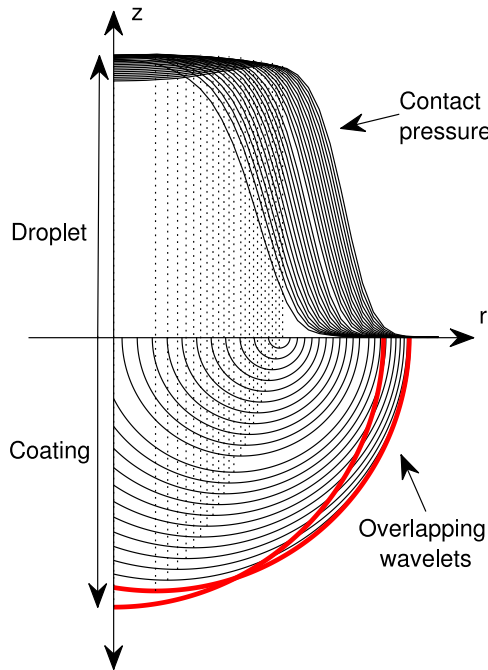

Fig. 16. Overlapping of wavelets in the coating.

Table 3
Summary of the effect of each of the studied parameters on the stress magnitude and stress field size and shape.

Parameter	Maximum stress	Stress field size and shape
Impact velocity	+++	+
Droplet diameter	+	+++
Material parameters	++	++
Material model	+	+
LEP thickness	++	+++
Interphase thickness	++	+
Surface roughness & cracks	+++	only local
Voids and inclusions	+++	only local

It was shown that LEP thickness significantly influences the stress field due to interactions of the stress wave with interfaces/inclusions. For thicker coating layers, the energy in the wave has dispersed and the initial wave is causing the highest stress magnitude. Hence, an LEP thickness limit exists where the highest stress is no longer influenced by the LEP design. This thickness could be considered as a design limit for LEP design. This LEP thickness limit should also take into account droplet diameter since it was shown that larger droplets lead to a larger area with high stress. This is due to the overlapping wavelets in the coating as discussed previously. This is another indication that LEP design is highly dependent on the impact and material parameters and that site specific tailoring of the coating system is required.

The viscoelastic model is based on low strain rate properties but, as shown in the introduction, at high strain rates, polyurethane and polyurea materials behave in a glassy way with more linear elastic behavior and less viscoelasticity. In order to accurately study the importance of hyperelasticity and viscoelasticity, high strain rate material parameters should be obtained by e.g. a split Hopkinson pressure bar test (SHPB) or time–temperature superposition of dynamic mechanical thermal analysis (DMTA) results, which is valid if the active molecular motions at high strain rates are the same as for low temperatures. It is expected that most materials considered for LEP coatings behave glassy in the relevant strain rate regime and that the linear elastic model is sufficient for prediction of the elastic stress field.

The study on the effect of surface roughness, surface cracks and voids or other inclusions has shown stress concentrations around irregularities in the material. These stress concentrations arise due to interactions of the stress waves with the defects and not solely due to the lateral jets interacting with the surface defects directly. It was shown that a layer of air is present in between the impacting droplet and the substrate. This air layer causes cushioning of the impact pressures but also acts as a lubricant for the droplet to deform. The air layer causes the droplet to have limited interactions with the surface irregularities directly, although the effect of the level-set definition for the two-phase flow domain on the air layer thickness has to be further studied. The stress concentrations caused by interactions of the stress waves with surface or internal defects could lead to an earlier onset of damage, especially when considering fatigue damage. The presence of micro defects could therefore accelerate fatigue damage locally leading to premature failure of the LEP. It is recommended to further investigate the initial void content and presence of damage in order to optimize LEP performance. Moreover, the presence of filler particles or fibers affect the stress field. These effects should be further studied, especially regarding the glass fibers that are typically present in the substrate materials and the filler particles that are present in the coating layers.

5. Conclusions

The current paper presented a numerical framework for modeling the dynamic stress state in the coating substrate system for wind turbine blades due to liquid droplet impact by using the contact pressure load as input. The effect of changes in impact, geometric and material parameters on the stress field was studied using the developed model. The resulting stress fields could be used as input for lifetime prediction models in future work. It was found that the stress distribution depends heavily on the design of the coating system and the following conclusions were drawn:

1. Impact velocity and maximum occurring stress in the target due to liquid droplet impact are related in a quadratic fashion rather than a linear fashion.
   This contradicts the generally accepted Waterhammer equation and should be taken into account when considering lifetime predictions and interpreting rain erosion test results since it can be expected to lead to a better correlation between rain erosion test results and traditional fatigue experiments.

2. The interaction of the contact pressure with the coating material causes overlap of high stress regions. This causes the typical crescent stress field shape in the bulk material.

   If the problem is simplified to a discrete generation of wavelets, due to a constant generation of wavelets at the contact edge of the droplet and the substrate, overlap of wavelets occurs. This is due to the fact that the wavelets in the coating expand with the acoustic velocity and the contact radius increases with a non constant velocity. Since this effect depends on the contact radius velocity, it is also affected by impact velocity and droplet radius. This implies that an optimal coating system should be site specific in order to take these parameters into account.

3. A coating thickness limit exists where thicker coatings no longer reduce the maximum occurring stress.

   For thin coatings, the maximum occurring stress in the coating substrate system is determined by interactions of the initial stress wave with the interface. When thicker coating systems are applied, the wave has more time to disperse before interacting with the interface, leading to lower stress concentrations at the interface. At some coating thickness, the highest stress is no longer caused by interactions with the interface but by the initial incoming wave. This thickness is considered as the coating thickness limit to apply after which additional thickness is no longer beneficial for the stress state in the system. This limit can be determined by simulating a parameter sweep for LEP thickness. The effect of overlapping wavelets also influences the development of the wave in the system and therefore the coating thickness limit is also depending on impact velocity and droplet radius.

4. Functionally graded material properties across an interphase region could reduce the effect of stress concentrations at the interphase.

   Interactions at the coating substrate transition region cause stress concentrations in the system. A gradual transition of elastic properties over an interphase region could reduce the stress concentrations due to a more spread out interaction with the wave. This causes a longer time in which transmission and reflections occur leading to a lower energy density in the wave. This effect is especially beneficial for low coating thicknesses where interface effects play a major role in the stress state of the system.

5. An air layer is present between the droplet and the substrate reducing the contact pressures and limiting the direct interactions of the water with surface defects.

   The direct interaction of lateral jets from the droplet with surface defects is limited due to the air layer that is present which is acting as a lubrication layer. Moreover, this layer is reducing the contact pressures of the water on the substrate due to a cushioning effect. A further study into the effect of the two-phase flow definition on the behavior of this air layer is recommended. Also, the effect of the definition of the surface roughness and the interactions with the air layer on the resulting stress fields should be further studied.

6. Stress waves in the coating interact with defects and inclusions causing stress concentrations which could accelerate fatigue damage accumulation.

   Small defects in the material can act as fatigue damage nucleation points which could lead to a severe decrease in lifetime. In order to include defects in lifetime prediction models, three dimensional simulations should be performed where droplet impacts occur over a distributed area. This approach is computationally expensive but could lead to a better lifetime prediction because of a more detailed description of damage initiation.

The stress development in the coating substrate system is the result of an intricate balance between impact, geometrical and material parameters of the system. The current work analyzed the effect of these parameters on the dynamic stress field by utilizing a numerical modeling framework. The trends were discussed and explained by theoretical descriptions of the interactions between the impacting water droplet, the cushioning air layer and the coating system. The results form a first step towards an optimization framework and a definition for LEP design guidelines.

CRediT authorship contribution statement

T.H. Hoksbergen: Conceptualization, Methodology, Software, Formal analysis, Investigation, Data curation, Writing – original draft, Writing – review & editing, Visualization. **R. Akkerman:** Validation, Writing – review & editing, Supervision. **I. Baran:** Conceptualization, Validation, Supervision, Project administration, Funding acquisition.

Declaration of competing interest

The authors declare that they have no known competing financial interests or personal relationships that could have appeared to influence the work reported in this paper.

Acknowledgments

Appendix A. Supplementary data

Supplementary material related to this article can be found online at https://doi.org/10.1016/j.renene.2023.119328.

References

[1] M.H. Keegan, D.H. Nash, M.M. Stack, On erosion issues associated with the leading edge of wind turbine blades, J. Phys. D: Appl. Phys. 46 (38) (2013) 383001, http://dx.doi.org/10.1088/0022-3727/46/38/383001.

[2] E.F. Tobin, T.M. Young, D. Raps, O. Rohr, Comparison of liquid impingement results from whirling arm and water-jet rain erosion test facilities, Wear 271 (9–10) (2011) 2625–2631, http://dx.doi.org/10.1016/j.wear.2011.02.023.

[3] N. Li, Q. Zhou, X. Chen, T. Xu, S. Hui, D. Zhang, Liquid drop impact on solid surface with application to water drop erosion on turbine blades, Part I: Nonlinear wave model and solution of one-dimensional impact, Int. J. Mech. Sci. 50 (10–11) (2008) 1526–1542, http://dx.doi.org/10.1016/J.IJMECSCI.2008.08.001.

[4] Q. Zhou, N. Li, X. Chen, T. Xu, S. Hui, D. Zhang, Liquid drop impact on solid surface with application to water drop erosion on turbine blades, Part II: Axisymmetric solution and erosion analysis, Int. J. Mech. Sci. 50 (10–11) (2008) 1543–1558, http://dx.doi.org/10.1016/J.IJMECSCI.2008.08.002.

[5] J.P. Dear, J.E. Field, High-speed photography of surface geometry effects in liquid/solid impact, J. Appl. Phys. 63 (4) (1988) 1015–1021, http://dx.doi.org/10.1063/1.340000.

[6] M.H. Keegan, D.H. Nash, M.M. Stack, Modelling rain drop impact of offshore wind turbine blades, Proc. ASME Turbo Expo 6 (2012) 887–898, http://dx.doi.org/10.1115/GT2012-69175.

[7] S. Doagou-Rad, L. Mishnaevsky, Rain erosion of wind turbine blades: Computational analysis of parameters controlling the surface degradation, Meccanica 55 (4) (2020) 725–743, http://dx.doi.org/10.1007/s11012-019-01089-x.

[8] T.H. Hoksbergen, R. Akkerman, I. Baran, Liquid droplet impact pressure on (elastic) solids for prediction of rain erosion loads on wind turbine blades, J. Wind Eng. Ind. Aerodyn. 233 (2023) 105319, http://dx.doi.org/10.1016/j.jweia.2023.105319.

[9] R.M. Blowers, On the response of an elastic solid to droplet impact, IMA J. Appl. Math. 5 (2) (1969) 167–193, http://dx.doi.org/10.1093/imamat/5.2.167.

[10] E. Cortés, F. Sánchez, A. O'Carroll, B. Madramany, M. Hardiman, T.M. Young, On the material characterisation of wind turbine blade coatings: The effect of interphase coating-laminate adhesion on rain erosion performance, Materials 10 (10) (2017) 1146, http://dx.doi.org/10.3390/ma10101146.

[11] J.S.M. Zanjani, I. Baran, Co-bonded hybrid thermoplastic-thermoset composite interphase: Process-microstructure-property correlation, Materials 14 (2) (2021) 1–17, http://dx.doi.org/10.3390/ma14020291.

[12] J.S. Monfared Zanjani, I. Baran, R. Akkerman, Characterization of interdiffusion mechanisms during co-bonding of unsaturated polyester resin to thermoplastics with different thermodynamic affinities, Polymer 209 (2020) 122991, http://dx.doi.org/10.1016/j.polymer.2020.122991.

[13] G. Ribeiro Salomão, H. Gojzewski, O. Erartsin, I. Baran, Novel co-bonded thermoplastic elastomer-epoxy/glass hybrid composites: The effect of cure temperature on the interphase morphology, Polym. Test. 115 (2022) 107736, http://dx.doi.org/10.1016/j.polymertesting.2022.107736.

[14] G.S. Springer, Erosion By Liquid Impact, John Wiley and Sons, New York, NY, 1976, p. 264.

[15] H.M. Slot, E.R.M. Gelinck, C. Rentrop, E. Van der Heide, Leading edge erosion of coated wind turbine blades: Review of coating life models, Renew. Energy 80 (2015) 837–848, http://dx.doi.org/10.1016/j.renene.2015.02.036.

[16] B. Amirzadeh, A. Louhghalam, M. Raessi, M. Tootkaboni, A computational framework for the analysis of rain-induced erosion in wind turbine blades, part II: Drop impact-induced stresses and blade coating fatigue life, J. Wind Eng. Ind. Aerodyn. 163 (February) (2017) 44–54, http://dx.doi.org/10.1016/j.jweia.2016.12.007.

[17] B. Amirzadeh, A. Louhghalam, M. Raessi, M. Tootkaboni, A computational framework for the analysis of rain-induced erosion in wind turbine blades, part I: Stochastic rain texture model and drop impact simulations, J. Wind Eng. Ind. Aerodyn. 163 (November 2016) (2017) 33–43, http://dx.doi.org/10.1016/j.jweia.2016.12.006.

[18] S. Doagou-Rad, L. Mishnaevsky, J.I. Bech, Leading edge erosion of wind turbine blades: Multiaxial critical plane fatigue model of coating degradation under random liquid impacts, Wind Energy 23 (8) (2020) 1752–1766, http://dx.doi.org/10.1002/we.2515.

[19] W. Hu, W. Chen, X. Wang, Z. Jiang, Y. Wang, A.S. Verma, J.J. Teuwen, A computational framework for coating fatigue analysis of wind turbine blades due to rain erosion, Renew. Energy 170 (2021) 236–250, http://dx.doi.org/10.1016/j.renene.2021.01.094.

[20] N. Hoksbergen, R. Akkerman, I. Baran, The springer model for lifetime prediction of wind turbine blade leading edge protection systems: A review and sensitivity study, Materials 15 (3) (2022) 1170, http://dx.doi.org/10.3390/ma15031170.

[21] L. Mishnaevsky, J. Sütterlin, Micromechanical model of surface erosion of polyurethane coatings on wind turbine blades, Polym. Degrad. Stab. 166 (2019) 283–289, http://dx.doi.org/10.1016/j.polymdegradstab.2019.06.009.

[22] D. Pedrazzoli, I. Manas-Zloczower, Understanding phase separation and morphology in thermoplastic polyurethanes nanocomposites, Polymer 90 (2016) 256–263, http://dx.doi.org/10.1016/j.polymer.2016.03.022.

[23] J. Yi, M.C. Boyce, G.F. Lee, E. Balizer, Large deformation rate-dependent stress–strain behavior of polyurea and polyurethanes, Polymer 47 (1) (2006) 319–329, http://dx.doi.org/10.1016/j.polymer.2005.10.107.

[24] J.I. Bech, N.F.J. Johansen, M.B. Madsen, Á. Hannesdóttir, C.B. Hasager, Experimental study on the effect of drop size in rain erosion test and on lifetime prediction of wind turbine blades, Renew. Energy 197 (January) (2022) 776–789, http://dx.doi.org/10.1016/j.renene.2022.06.127.

[25] A.S. Verma, Z. Jiang, M. Caboni, H. Verhoef, H. van der Mijle Meijer, S.G.P. Castro, J.J.E. Teuwen, A probabilistic rainfall model to estimate the leading-edge lifetime of wind turbine blade coating system, Renew. Energy 178 (2021) 1435–1455, http://dx.doi.org/10.1016/j.renene.2021.06.122.

[26] J.C. López, A. Kolios, L. Wang, M. Chiachio, A wind turbine blade leading edge rain erosion computational framework, Renew. Energy 203 (December 2022) (2023) 131–141, http://dx.doi.org/10.1016/j.renene.2022.12.050.

[27] L. Mishnaevsky, C.B. Hasager, C. Bak, A.-M. Tilg, J.I. Bech, S. Doagou Rad, S. Fæster, Leading edge erosion of wind turbine blades: Understanding, prevention and protection, Renew. Energy 169 (2021) 953–969, http://dx.doi.org/10.1016/j.renene.2021.01.044.

[28] T.H. Hoksbergen, R. Akkerman, I. Baran, Coating stress analysis for leading edge protection systems for wind turbine blades, in: Proceedings of the 20th European Conference on Composite Materials - Composites Meet Sustainability, Vol. 5, 2022, pp. 113–120, http://dx.doi.org/10.5075/epfl-298799_978-2-9701614-0-0.

[29] G.A. Holzapfel, Nonlinear Solid Mechanics: A Continuum Approach for Engineering, Wiley, 2000, p. 470.